Material: Ferritic Steel: F82H
Property: Stress Amplitude vs. Number of Cycles
Condition: Neutron Irradiation, Helium Implantation
Data: Experimental

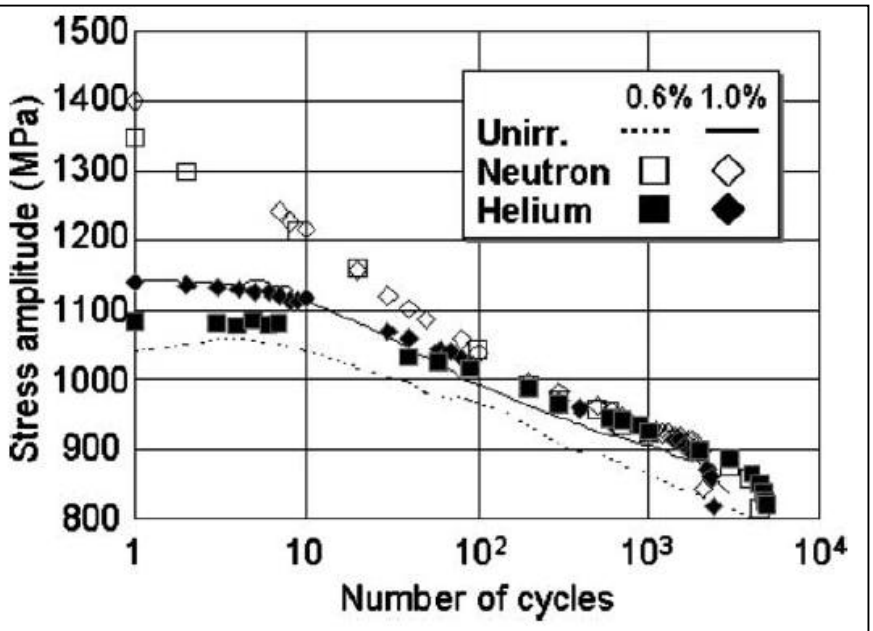

Fig. 4. Cyclic stress response curves. All specimens showed continuous cyclic softening behavior. However, the helium ion implanted samples showed stable stress amplitude in the initial cycles.

Source:
Journal of Nuclear Materials 307-311 (2002) 304-307

Title of paper (or report) this figure appeared in:
Radiation Effects on Low Cycle Fatigue Properties of Reduced Activation Ferritic/Martensitic Steels

Author of paper or graph:
T. Hirose, H. Tanigawa, M. Ando, A. Kohyama, Y. Katoh, M. Narui,

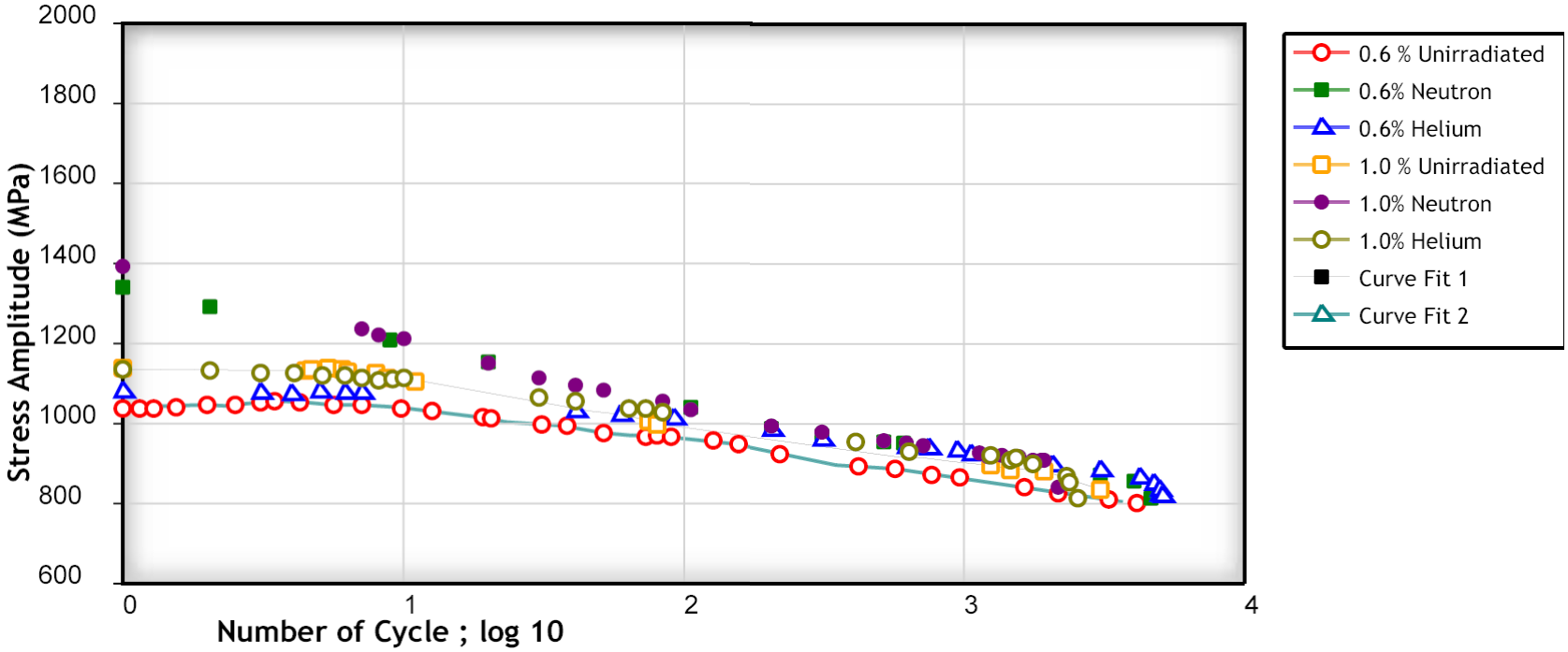

Cyclic stress response curves. All specimens showed continuous cyclic softening behavior. However, the helium ion implanted samples showed stable stress amplitude in the initial cycles.

Reference:

Author: *T. Hirose, H. Tanigawa, M. Ando, A. Kohyama, Y. Katoh, M. Narui,*

Title: *Radiation Effects on Low Cycle Fatigue Properties of Reduced Activation Ferritic/Martensitic Steels*

Source: *Journal of Nuclear Materials, 2002, Volume 307-311, Page 304-307*, [PDF]

View Data

Author Comments

Plot Format:

Y-Scale: ◉ linear ○ log ○ ln

ELSEVIER

Journal of Nuclear Materials 307–311 (2002) 304–307

journal of nuclear materials

www.elsevier.com/locate/jnucmat

Radiation effects on low cycle fatigue properties of reduced activation ferritic/martensitic steels

T. Hirose [a,*], H. Tanigawa [b], M. Ando [b], A. Kohyama [a], Y. Katoh [a], M. Narui [c]

[a] *Institute of Advanced Energy, Kyoto University, Gokasho, Uji, Kyoto 611-0011, Japan*
[b] *Japan Atomic Energy Research Institute, 2-4 Shirakata, Tokai-Mura, Naka-Gun, Ibaraki 319-1195, Japan*
[c] *Institute for Materials Research, Tohoku University, Naritamachi Oarai, Higashi-Ibaraki, Ibaraki 311-1313, Japan*

Abstract

The reduced activation ferritic/martensitic steel, RAFs F82H IEA heat has been fatigue-tested at ambient temperature under diametral strain controlled conditions. In order to evaluate the effects of radiation damage and transmutation damage on fatigue characteristics, post-neutron irradiation and post-helium ion implantation fatigue tests were carried out. Fracture surfaces and fatigue crack initiation on the specimen surface were observed by SEM. Low-temperature irradiation caused an increase in stress amplitude and a reduction in fatigue lifetime corresponding to radiation hardening and loss of ductility. Neutron irradiated samples showed brittle fracture surface, and it was significant for large strain tests. On the other hand, helium implantation caused delay of cyclic softening. However, brittle crack initiation and propagation did not depend on the helium concentration profiles.

1. Introduction

Reduced activation ferritic/martensitic steels (RAFs) are the leading candidates for the blanket first wall structural materials of the D–T fusion reactors. In fusion applications, the structural materials will suffer from not only the radiation damage and but also transmutation damage. The transmutation damage, especially helium from (n, α) reactions might be considered to degrade ductility of RAFs [1]. Furthermore, the structural materials will be also exposed to cyclic stresses caused by reactor operation. However, fatigue properties of neither unirradiated nor irradiated RAFs have not been clarified yet. It was reported that $\sim$100 appm of helium imposed significant effects on impact properties of ^{10}B-doped steels [2]. On the other hands, $\sim$700 appm helium implantation using a cyclotron accelerator did not cause any degradation in small punch properties [3]. The effect of transmutation induced helium on RAFs fatigue properties have not been studied yet. The objective of this work is to evaluate the effect of neutron irradiation and helium generation on low cycle fatigue properties of RAFs F82H IEA heat. F82H IEA heat has been fatigue tested at ambient temperature under diametral strain-controlled conditions. In order to evaluate the effects of radiation damage and transmutation damage on fracture characteristics, fatigue tests were carried out following neutron irradiation and helium ion implantation.

2. Experimental procedure

The material used was F82H IEA heat. The chemical composition is given in [4]. The plate was 25 mm thick and was heat-treated as follows: Normalizing (1313 K/40 min/air cooled) and Tempering (1020 K/30 min/air cooled). It is well known that the hourglass type specimen has good resistance to buckling, which is a very

* Corresponding author. Address: Department of Fusion Engineering Research, Blanket Engineering Laboratory, Japan Atomic Energy Research Institute, 801-1 Mukoyama, Naka-Machi, Naka-Gun, Ibaraki 311-0193, Japan. Tel.: +81-29 270 7570; fax: +81-29 270 7489.

E-mail address: hiroset@fusion.naka.jaeri.go.jp (T. Hirose).

0022-3115/02/$ - see front matter
PII: S0022-3115(02)01199-6

important issue in miniaturizing specimens for push–pull tests. Moreover it is necessary for ion implantation experiments, because fracture initiation site was limited to around the specimen's minimum diameter portion. Miniaturized hourglass specimen SF-1 was used in this work [5]. Volume that can be irradiated with ions is very limited as is the volume that is deformed into an hourglass specimen. The shape and dimension of the specimens are presented in Fig. 1. SF-1 specimen is proposed to be used in accelerator driven D–Li neutron sources, such as the international fusion materials irradiation facility. The specimens were machined from the 25-mm thick plate. The rolling direction was parallel to specimens' longitudinal direction.

The neutron irradiation on SF-1 specimen was carried out using the Japan materials testing reactor (JMTR) in the Japan Atomic Energy Research Institute (JAERI). The specimen was irradiated to 0.02 dpa at temperature below 363 K.

In parallel with the neutron irradiation, helium ion implantation using AVF cyclotron accelerator was performed at a JMTR equivalent temperature of ~393 K with a degraded 50 MeV α-particle beam. Aluminum energy degrader wheel was applied to achieve a homogeneous helium concentration profile. The degrader consists of 32 pieces of aluminum foil with different thicknesses. The amount of implanted helium was calculated by TRIM-98 code. The depth profile of implanted helium and displacement damage are presented in Fig. 2. As shown in this figure, the helium distribution range was not enough for SF-1 fatigue specimen. Therefore the α-particle was implanted from two sides of SF-1 specimen. The neutron irradiation and helium implantation conditions are summarized in Table 1.

Low cycle fatigue tests were carried out at the ambient temperature and in air in strain diametral controlled mode. The laser extensometer was used for monitoring of the diametral deformation, it enabled the measurement without any contacts on the specimen

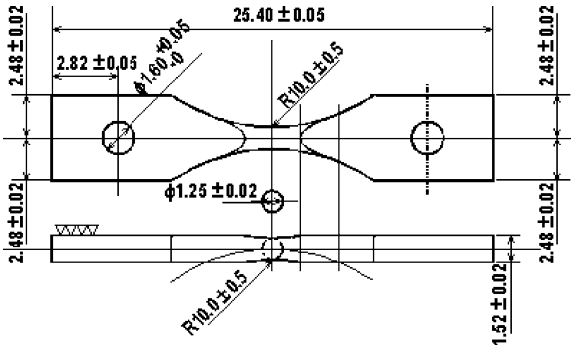

Fig. 1. Dimension of miniaturized hourglass shaped fatigue specimen.

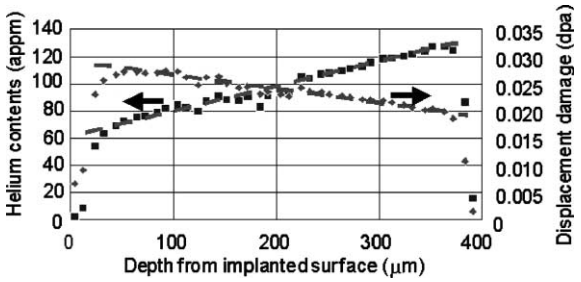

Fig. 2. The depth profile of implanted helium and displacement damage calculated by TRIM-98 code.

Table 1
Parameters of the neutron irradiation and helium implantation

	Neutron irradiation	Helium implantation
Irradiation temperature	~363 K	~393 K
Displacement damage rate	$\sim 3.9 \times 10^{-8}$ dpa/s	$\sim 7.0 \times 10^{-7}$ dpa/s
Helium/displacement	$\sim 1.0 \times 10^{-2}$ appm/dpa	$\sim 4.5 \times 10^{3}$ appm/dpa
Nominal helium contents	2.0×10^{-4} appm	120 appm
Nominal displacement damage	0.02 dpa	0.03 dpa

surface [6]. A completely push–pull condition was applied, and the total strain range was controlled with a diametral strain rate 0.04%/s. After the mechanical tests, SEM observations on the fracture surface were carried out.

To evaluate the magnitude of irradiation hardening, miniaturized tensile specimens were also neutron irradiated and helium ion implanted. The specimen used was SS-J type sheet tensile specimen. The cross section of the specimen was 1.2 mm × 0.3 mm, and the gauge length was 5 mm. Tensile tests were carried out at the ambient temperature and in air with 0.07%/s strain rate.

3. Results and discussions

3.1. Radiation effects on fatigue properties

Tensile tests revealed that the irradiation with neutron and implantation with α-particle caused the same level of irradiation hardening, and the increase in the strength was not affected by irradiation particles. The increase in 0.2% proof stress and ultimate tensile stress were 100 and 60 MPa, respectively. The fracture surface of neutron irradiated sample showed smaller reduction in area than the unirradiated sample and helium implanted sample. It is considered that irradiation

hardening in this work was caused only by the displacement damage and the implanted helium did not cause significant degradation of ductility.

The neutron irradiation and helium implantation effects on the fatigue lifetime are presented in Fig. 3. The total strain range is plotted as a function of the number of cycles to failure, N_f. As shown in this figure, the neutron irradiated samples showed the shortest lifetime. And the reduction of the N_f was significant for the large strain test condition.

The neutron and helium irradiation effects on the stress amplitudes are presented in Fig. 4. Total stress amplitude is plotted as a function of the number of cycles. The increase in the stress amplitude related to the radiation hardening was observed in the neutron-irradiated samples. On the other hands, helium implanted samples showed only small shifts in the stress amplitudes. The helium-implanted region were dominant in the specimens mid plane, however, as shown in Fig. 2, the helium contents at the other region were limited to beneath the surface. The small volume fraction of implanted region did not affect the stress amplitudes significantly. F82H demonstrated cyclic softening both before and after the irradiation. Fig. 5 shows the neutron irradiation and helium ion implantation on the cyclic softening behavior. The vertical axis represents the stress amplitude normalized by initial stress amplitude, and horizontal axis represents the number of cycles normalized by N_f. Previous work on microstructural analysis on fatigue fractured RAFs revealed that cyclic softening of RAFs are caused by diminishing of lath structure and formation of cell structure [7,8]. The present results imply that the simple displacement damage induced by neutron irradiation seemed to be easily swept by dislocations [9]. However, the complexes of defect clusters and implanted helium restricts the formation of cell structure.

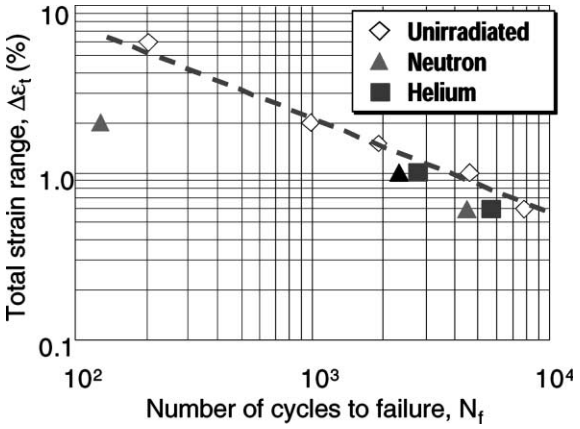

Fig. 3. The effects of neutron irradiation and helium implantation on the fatigue lifetime of F82H IEA heat.

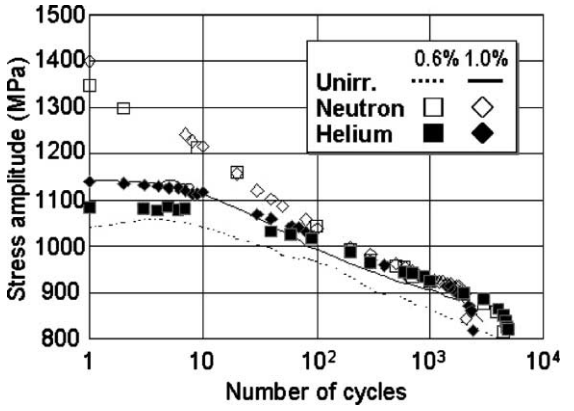

Fig. 4. Cyclic stress response curves. All specimens showed continuous cyclic softening behavior. However, the helium ion implanted samples showed stable stress amplitude in the initial cycles.

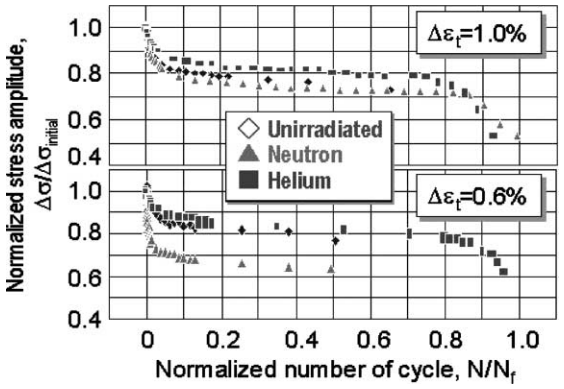

Fig. 5. Normalized cyclic stress response curves.

3.2. Fracture appearance

Fatigue striation pattern was observed on the fracture surface of unirradiated samples. Many cracks emerged on the specimen's side surface [7]. These cracks initiated along with prior-austenite grain boundaries [9]. Fig. 6 showed fracture surface of neutron irradiated samples. As shown in this figure, crack initiated in a brittle manner. Local brittle fracture was observed in the middle of the fracture surface. The brittle fractured increased with total strain range. In case of 1.0% or 0.6% tests, the fatigue fracture proceeded in ductile manner in total. These results imply that the reduction in N_f was caused by the local brittle crack propagation.

The fracture surfaces of helium ion implanted samples are presented in Fig. 7. The fracture surface was similar to that of the neutron irradiated samples. The crack initiation occurred at the minimum diameter plane. The plane contained helium concentration pro-

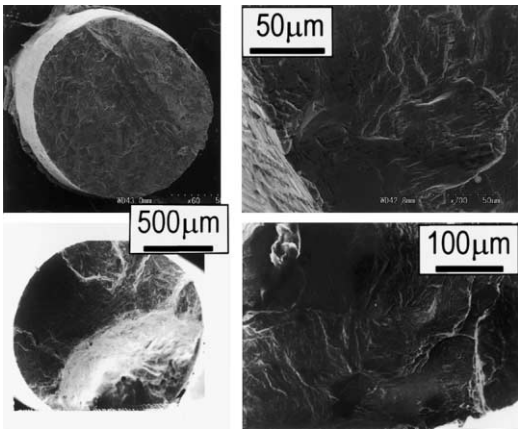

Fig. 6. Fracture Surfaces of neutron irradiated samples. Upper: $\Delta\varepsilon_t = 1.0\%$, $N_f = 2.3 \times 10^3$ and lower: $\Delta\varepsilon_t = 2.0\%$, $N_f = 1.3 \times 10^2$.

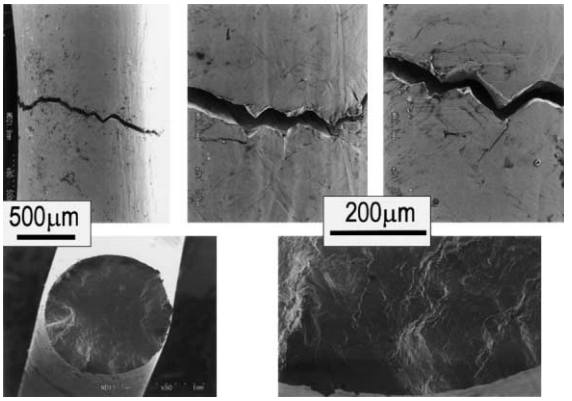

Fig. 7. Fracture Surfaces of helium implanted samples. Upper: $\Delta\varepsilon_t = 1.0\%$, $N_f = 2.8 \times 10^3$ and lower: $\Delta\varepsilon_t = 0.6\%$, $N_f = 7.9 \times 10^3$.

files presented in Fig. 2, however fracture appearance seemed not to be affected by the helium concentration. It is reported that F82H with 400 appm helium showed intergranular cracking [10]. However, intergranular crack initiation was not observed in this work. It is reported that the implanted helium was trapped at the high density dislocations of the martensite lath structure [11]. It is considered that the capacity of dislocations for trapping helium was enough to trap the 120 appm implanted helium.

4. Summary

Tensile and fatigue specimens were irradiated to a dose level of 0.02 dpa at temperature below 363 K and helium-ion-implanted to a level of 120 appm at temperature below 393 K.

1. The irradiation and implantation caused irradiation hardening. The stress range of fatigue tests reflected this hardening. However, all samples showed cyclic softening, the simple displacement damage seemed to be easily swept by dislocations.
2. The helium-ion-implanted samples showed blunt cyclic softening behavior. The implanted helium is considered to restrict the cell structure formation.
3. Fatigue cracks were initiated along with prior-austenite grain boundaries. The initiation behavior was not affected by the neutron irradiation and the helium ion implantation, however, the crack propagation properties were locally changed to brittle type.
4. The reduction in N_f caused by neutron irradiation was significant. The reduction was caused by local brittle fracture. The brittle fractured area increased with strain range.

Acknowledgements

The authors would like to express their sincere appreciation to Professor Namba, Professor Nishimura, Professor Muroga and Dr Nagasaka of NIFS, Dr Shiba, Dr Miwa and Dr Jitsukawa of JAERI for their useful help in many aspects of this work. They are grateful to Institute for Materials Research, Tohoku University, for facilitating post-irradiation experiments.

References

[1] S. Jitsukawa, ASTM STP 1125 (1992) 1083.
[2] K. Shiba, A. Hishinuma, J. Nucl. Mater. 283–287 (2000) 474.
[3] R. Kasada, T. Morimura, A. Hasegawa, A. Kimura, J. Nucl. Mater., in press.
[4] A. Hishinuma, A. Kohyama, R.L. Klueh, D.S. Gelles, W. Dietz, K. Ehrlich, J. Nucl. Mater. 258–263 (1998) 193.
[5] T. Hirose, H. Sakasegawa, A. Kohyama, Y. Katoh, H. Tanigawa, J. Nucl. Mater. 283–283 (2000) 1018.
[6] C. Brillaud, T. Meylogan, P. Salathe, ASTM STP 1270 (1996) 1144.
[7] T. Hirose, H. Tanigawa, M. Ando, A. Kohyama, Y. Katoh, S. Jitsukawa, Mater. Trans. JIM 43 (2000) 389.
[8] T. Hirose, H. Tanigawa, M. Ando, T. Suzuki, A. Kohyama, Y. Katoh, M. Narui, ASTM STP 1418, in press.
[9] Tanigawa, T. Hirose, M. Ando, S. Jitsukawa, Y. Katoh, A. Kohyama, these Proceedings.
[10] J. Bertsch, S. Meyer, A. Möslang, J. Nucl. Mater. 283–287 (2000) 832.
[11] R. Sugano et al., these Proceedings.